IEEE Access
Multidisciplinary | Rapid Review | Open Access Journal

Received April 19, 2019, accepted May 27, 2019, date of publication May 31, 2019, date of current version June 12, 2019.

Digital Object Identifier 10.1109/ACCESS.2019.2920245

Hardware-in-the-Loop Simulation for Active Control of Tramcars With Independently Rotating Wheels

YE JUN OH[1], JAE-KWANG LEE[1], HUAI-CONG LIU[1], SOOYOUNG CHO[1], JU LEE[1], (Senior Member, IEEE), AND HO-JOON LEE[2]

[1]Department of Electrical Engineering, Hanyang University, Seoul 04763, South Korea
[2]Department of Electric Automatization, Busan Institute of Science Technology University, Busan 46639, South Korea

Corresponding author: Ho-Joon Lee (hjlee@bist.ac.kr)

This work was supported in part by the Ministry of Trade, Industry, and Energy, South Korea through the Human Resources Program in Energy Technology of the Korea Institute of Energy Technology Evaluation and Planning under Grant 20174030201750, and in part by Basic Science Research Program through the National Research Foundation of Korea (NRF) funded by the Ministry of Education, Science and Technology under NRF-2017R1D1A1B03032635.

ABSTRACT The wheelset is an important part that affects the dynamics of railway vehicles. The main purpose of the wheelset is to solve the problem of stability, curve performance, comfort, and wear. A conventional railway vehicle adopts rigid-axle wheelset (RW) due to the self-centering mechanism. On the other hand, independently rotating wheels (IRWs) have not been widely applied in the railway industry, since they do not generate any self-centering mechanism. It creates excessive wear, and derailment may occur. However, the IRWs have excellent curving performance compared with the RWs, and it enables realizing a low-floor structure that is convenient for passengers to get on and off. The recent active control technology has made it possible to generate a centering force in the IRWs. There are still many obstacles for the practical use of this technology, and it is necessary to verify the control strategies through various test methods. In this paper, an analytical model is derived, and an active control strategy is studied. To verify the validity of the active control strategy, a novel hardware-in-the-loop simulation (HILS) configuration using a real-time model and a motor–generator set are proposed.

INDEX TERMS Active control, hardware-in-the-loop simulation (HILS), motor control, independently rotating wheels (IRWs), railway vehicle, rigid-axle wheelset (RW).

I. INTRODUCTION

In the electrical industry, high-voltage conversion is required for efficient transmission. To meet this requirement, there was ''the war of currents'' between the alternating current (AC) and direct current (DC) distribution system. The war ended when the AC distribution system was adopted. The main reason the AC became victorious was the invention of the transformer, which could easily convert high-voltage without additional control [1], [2].

The railway industry also has a similar history as that of the electrical industry. The wheelset of railway vehicles requires restoration capability when there is a misalignment between the wheels and rails, in order to improve safety and efficiency. Traditionally wheelsets have been categorized as either rigid-axle wheelset (RW) or independently rotating wheels (IRWs) [3]. Since the conical wheel of RW made it possible to generate the self-centering ability, RW have been adopted in most railway vehicles. It is mainly studied with regard to traction torque control [4]–[6]. From this perspective, RW is a fascinating mechanical component. However, it has several inherent problems such as instability at high speeds and severe friction in the curved track [7], [8].

IRWs have been studied to solve these problems. Since IRWs allow for speed difference between the left and right wheels, the longitudinal creep is removed. This improves stability and the curving performance. Moreover, since there is no central axle between two wheels in IRWs, the vehicle has a lower height, making it convenient for passengers to get on and off. As a result, IRWs are suitable for low-floor tramcars that run on tracks with sharp curved tracks in urban areas. However, it is vulnerable to disturbances on straight

The associate editor coordinating the review of this manuscript and approving it for publication was Emanuele Crisostomi.

tracks because the self-centering phenomenon disappears due to the removal of longitudinal creep. This creates a large amount of friction and noise between the wheels and the rail, which may result in derailment [9].

Many studies have been conducted to overcome the shortcomings of IRWs. Recent developments in power electronics and control technology have enabled active control that is capable of generating centering ability in IRWs. In previous studies, it was implemented by applying an additional actuator (yaw torque or lateral force) between the body and the wheelset. Since the lateral actuator degrades the ride quality, the yaw actuator has been preferred [10].

Mei conducted a study on the design of independent controllers, optimal controls, and sensors in terms of commercialization [11]–[14]. Zhao and Liang studied the re-adhesion control for a railway vehicles [15]. A study on the assessment stability and active guidance of railway vehicles was conducted by Goodall and Powell [16], [17]. Lu *et al.* studied a robust active controller to handle the uncertainty and nonlinear characteristics [18].

Railway vehicles with IRWs have a different platform from that of conventional railway vehicles, which significantly increases the cost of producing the test vehicle. To adapt active control technology for practical use, their feasibility should be verified appropriately. Therefore, it is necessary to develop a test method that reflects the characteristics of the controller and IRWs more accurately.

The test methods for verifying the active control strategy can be classified as shown in Table 1. In most previous studies, the effectiveness of the control strategy was evaluated using a linear analytic model [11]–[13]. In addition, a non-linear model was also used with the SIMPACK-MATLAB/Simulink interface [18]. However, since the numerical model is based on simulation, it does not consider hardware characteristics such as a real controller.

To solve these problems, an open-loop test method was proposed to verify the performance of the real controller (motor-inverter) [19], [20]. Lee performed scale-vehicle tests (1/5 scale vehicle with roller rig) using a laser type lateral displacement sensor [21], [22]. However, the drawback of scale-vehicles is that they have no similarity with a real vehicle in terms of dynamics.

Therefore, the test method using HILS can be a solution. In general, the HILS test can shorten the development time, prevent failures in the design process, avoid inaccuracies in simulation, and reduce the complexity and risk of the vehicle test. This method also considers irregular conditions such as failure as well as normal operation, thereby preventing human accidents. Despite these advantages, the active control of IRWs using HILS has rarely been studied.

In this paper, an active control strategy of IRWs is studied. To verify the validity of this control strategy, a novel HILS configuration and a test method using a real-time model and a motor–generator set are proposed.

The dynamic model of a railway vehicle with IRWs is described in Section II. The active control strategy and the novel HILS are studied in Sections III and IV, respectively. The driving scenarios and test environments are described in Section V, and the active control is verified through HILS test in Section VI.

II. DYNAMIC MODEL OF TRAMCARS WITH IRWS

This section studies a vehicle dynamics model with IRWs for real-time calculation. In order to analyze the dynamic model of a railway vehicle and to design a controller, it is necessary to understand the wheel-rail contact mechanism and the wheelset model accurately. This model is a function of space (x, y, z) and time (t). Since partial differential equations are used to solve the dynamic equation, the calculation is complicated and requires a very long time. A study comparing an analytical linear model with a non-linear full model using a multibody simulation package 'Simpack' has shown that an analytical linear model is quite suitable for the development of active controllers [12]. For this reason, the analytical model has been widely used [9], [23]. In this section, the vehicle models include effects of longitudinal motion, which have been ignored in previous analytical models of IRWs. This model is simple and more suitable for the proposed HILS environments.

A. WHEELSET MODEL

The dynamic model of a railway vehicle is based on the wheelset model. It is important to define the wheelset model because it extends to the bogie and vehicle models. One wheel can be expressed in 6 degrees of freedom (DOF) (i.e., x, y, z, ϕ, θ, and Ψ), and a wheelset consists of two wheels. However, when a wheelset is expressed using 12 DOF, the overall vehicle model becomes very complicated, and therefore it should be minimized. In order to deal with the active control strategies of IRWs, the dynamic equation may omit DOF that are unrelated to the restoration mechanism.

In the case of RW, the two wheels are joined by the central axle, and it acts as a single wheel. Therefore, it is possible to reduce the 12 DOF into 6 DOF. Since the time constant of the vehicle is large, the vehicle speed can be assumed to be constant. Therefore, the x-axis direction (forward motion) can be omitted. Moreover, the left and right wheels rotate at the same speed ($\dot{\theta}_L = \dot{\theta}_R$). Because no yaw moment is generated by the wheel speed, θ can be omitted from the wheelset model; z and ϕ can also be omitted because they do not affect the restoration mechanism. As a result, the wheelset model of RW is expressed by using only 2 DOF (Ψ, y) as shown Fig. 1(a).

In IRWs, yaw moments occur because the left and right wheels can have different speeds ($\dot{\theta}_L \neq \dot{\theta}_R$). It produces a restoration mechanism, and therefore θ_L and θ_R cannot be omitted from the wheelset model of IRWs. Since the speeds of the left and right wheels can be defined as a single variable ($\dot{\theta} = \left(\dot{\theta}_L - \dot{\theta}_R\right)/2$), the wheelset model can be expressed using 3 DOF (y, Ψ, θ). It is used primarily in the field of vehicle dynamics.

TABLE 1. Comparison between test methods.

	Off-line simulation	Scale-vehicle test	HILS test	Vehicle test
Vehicle model	Mathematical model	Scale-vehicle	Mathematical model	Real Vehicle
Controller model	Mathematical model	Scale-controller	Real controller	Real controller
Run time	Much longer than real time	Real time	Real time	Real time
Test condition alterations	Fully possible & easy	Limited & Difficult	Fully possible & easy	Limited & Difficult
Test repeatability	Fully possible & easy	Limited	Fully possible & easy	Limited
Development duration	Short	Less than vehicle test	Short	Long
Development cost	Less than HILS test	Less than vehicle test	Less than vehicle test	High

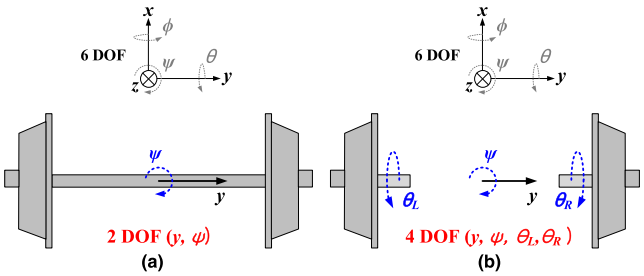

FIGURE 1. Wheelset model (a) RW (b) IRWs.

However, in the case of independent torque control of each wheel, the wheel speed cannot be expressed as a single variable. The speeds of the left and right wheels must be expressed using an independent variable (θ_L, θ_R). Therefore, the wheelset model of IRWs is represented using 4 DOF (y, Ψ, θ_L, θ_R) as shown in Fig. 1(b). The leading and trailing wheelset models are expressed as (1)-(4) and (5)-(8), respectively.

1) LEADING WHEELSET MODEL

$$\begin{aligned} m_w\ddot{y}_1 &= (-\frac{w\lambda}{a} - 2K_{py})y_1 + (\frac{-2f_{11}}{v} - \frac{-2f_{11}}{v}\frac{r_0}{a}\lambda - 2C_{py})\dot{y}_1 \\ &\quad + 2f_{11}\psi_1 - \frac{2f_{12}}{v}\dot{\psi}_1 + 2K_{py}y_b + 2C_{py}\dot{y}_b \\ &\quad + 2K_{py}L_1\psi_b + 2C_{py}L_2\dot{\psi}_b \qquad (1) \\ I_{wz}\ddot{\psi}_1 &= -2a\frac{\lambda}{r_0}f_{33}y_1 + (\frac{2f_{12}}{v} - I_{wy}\frac{v}{r_0}\frac{\lambda}{a} + 2f_{12}\frac{r_0}{v}\frac{\lambda}{a})\dot{y}_1 \\ &\quad + (-2f_{12} + a\lambda w - 2K_{px}b_1^2)\psi_1 \\ &\quad + (-2a^2\frac{f_{33}}{v} - \frac{2f_{22}}{v} - 2C_{px}b_1^2)\dot{\psi}_1 \\ &\quad + f_{33}a\frac{r_0}{v}\dot{\theta}_{1L} - f_{33}a\frac{r_0}{v}\dot{\theta}_{1R} + 2K_{px}b_1^2\psi_b + 2C_{px}b_1^2\dot{\psi}_b \\ &\qquad (2) \end{aligned}$$

$$I_{w1}\ddot{\theta}_{1L} = f_{33}\lambda y_1 + r_0 f_{33}\frac{a}{v}\dot{\psi}_1 - f_{33}\frac{r_0^2}{v}\dot{\theta}_{1L} \qquad (3)$$

$$I_{w1}\ddot{\theta}_{1R} = -f_{33}\lambda y_1 - r_0 f_{33}\frac{a}{v}\dot{\psi}_1 - f_{33}\frac{r_0^2}{v}\dot{\theta}_{1R} \qquad (4)$$

2) TRAILING WHEELSET MODEL

$$\begin{aligned} m_w\ddot{y}_2 &= (-\frac{w\lambda}{a} - 2K_{py})y_2 + (\frac{-2f_{11}}{v} - \frac{-2f_{11}}{v}\frac{r_0}{a}\lambda - 2C_{py})\dot{y}_2 \\ &\quad + 2f_{11}\psi_2 - \frac{2f_{12}}{v}\dot{\psi}_2 + 2K_{py}y_b + 2C_{py}\dot{y}_b \\ &\quad - 2K_{py}L_1\psi_b - 2C_{py}L_2\dot{\psi}_b \qquad (5) \\ I_{wz}\ddot{\psi}_2 &= -2a\frac{\lambda}{r_0}f_{33}y_2 + (\frac{2f_{12}}{v} - I_y\frac{v}{r_0}\frac{\lambda}{a} + 2f_{12}\frac{r_0}{v}\frac{\lambda}{a})\dot{y}_2 \\ &\quad + (-2f_{12} + a\lambda w - 2K_{px}b_1^2)\psi_2 \\ &\quad + (-2a^2\frac{f_{33}}{v} - \frac{2f_{22}}{v} - 2C_{px}b_1^2)\dot{\psi}_2 \\ &\quad + f_{33}a\frac{r_0}{v}\dot{\theta}_{2L} - f_{33}a\frac{r_0}{v}\dot{\theta}_{2R} + 2K_{px}b_1^2\psi_b + 2C_{px}b_1^2\dot{\psi}_b \\ &\qquad (6) \end{aligned}$$

$$I_{w2}\ddot{\theta}_{2L} = f_{33}\lambda y_2 + r_0 f_{33}\frac{a}{v}\dot{\psi}_2 - f_{33}\frac{r_0^2}{v}\dot{\theta}_{2L} \qquad (7)$$

$$I_{w2}\ddot{\theta}_{2R} = -f_{33}\lambda y_2 - r_0 f_{33}\frac{a}{v}\dot{\psi}_2 - f_{33}\frac{r_0^2}{v}\dot{\theta}_{2R} \qquad (8)$$

B. BOGIE AND CAR MODEL

The bogie model should consider the effects of the bogie frame and the first suspension. It can be expressed as (9)-(10) by adding 2 DOF to the wheelset model. Therefore, the bogie model can be expressed using a total of 10 DOF (4 DOF + 4 DOF + 2 DOF).

The car model should also consider the effects of the car body and the secondary suspension. It can be expressed as (11)-(12) by adding 2 DOF to the bogie model. Therefore, the car model can be expressed using 12 DOF. Tramcars generally adopt 3– to 5–car modules rather than single modules. In this study, we consider a 3-car module and it is expressed using 26 DOF as shown in Fig. 2.

1) BOGIE MODEL

$$\begin{aligned} m_b\ddot{y}_b &= 2K_{py}y_1 + 2C_{py}\dot{y}_1 + 2K_{py}y_2 + 2C_{py}\dot{y}_2 \\ &\quad + \left(-4K_{py} - 2K_{sy}\right)y_b + \left(-4C_{py} - 2C_{sy2}\right)\dot{y}_b \qquad (9) \\ I_b\ddot{\psi}_b &= 2K_{py}L_1y_1 + 2C_{py}L_2\dot{y}_1 + 2K_{px}b_1^2\psi_1 + 2C_{px}b_1^2\dot{\psi}_1 \\ &\quad - 2K_{py}L_1y_2 - 2C_{py}L_2\dot{y}_2 + 2K_{px}b_1^2\psi_2 + 2C_{px}b_1^2\dot{\psi}_2 \\ &\quad + \left(-4K_{py}L_1^2 - 4K_{px}b_1^2 - 2K_{sx}b_2^2\right)\psi_b \\ &\quad + \left(-4C_{py}L_2^2 - 4C_{px}b_1^2 - 2C_{sx}b_3^2\right)\dot{\psi}_b \qquad (10) \end{aligned}$$

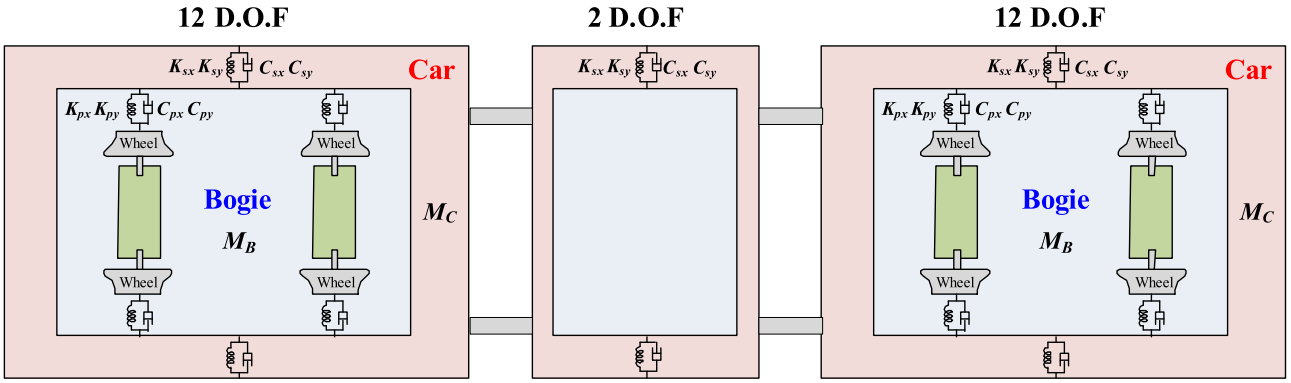

FIGURE 2. The analytical tramcars model (3 modules).

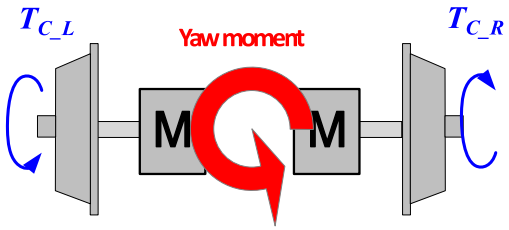

FIGURE 3. Generation of yaw moment through independent torque control.

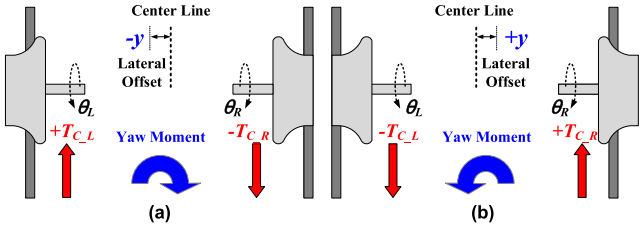

FIGURE 4. Active control strategy based on the lateral displacement (a) left-align (b) right-align.

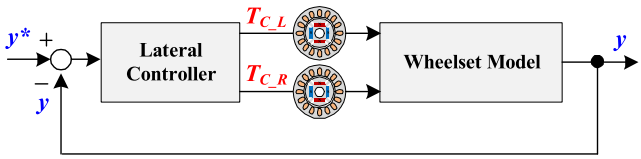

FIGURE 5. Block diagram of active controller.

2) CAR MODEL

$$\begin{aligned} m_{c1}\ddot{y}_{c1} &= 2K_{sy}y_{b1} - 2K_{sy}y_{c1} + 2C_{sy}\dot{y}_{b1} - 2C_{sy}\dot{y}_{c1} \\ &\quad - 2K_{sy}L_c\psi_{c1} - 2C_{sy}L_c\dot{\psi}_{c1} - K_{sy}y_{c1} + K_{sy}y_{c2} \\ &\quad - K_{sy}L_1\psi_{c1} - K_{sy}L_3\psi_{c2} \end{aligned} \tag{11}$$

$$\begin{aligned} I_{cz1}\ddot{\psi}_{c1} &= -2K_{sy}L_c^2\psi_{c1} - 2C_{sy}L_c^2\dot{\psi}_{c1} - 2K_{sx}L_1^2\psi_{c1} \\ &\quad - 2C_{sx}L_3^2\dot{\psi}_{c1} + 2K_{sx}L_1^2\psi_{b1} + 2C_{sx}L_3^2\dot{\psi}_{b1} \\ &\quad + 2K_{sy}L_cy_{b1} + 2C_{sy}L_c\dot{y}_{b1} + C_{sy}L_2\dot{y}_{c1} + K_{sy}L_2y_{c1} \\ &\quad + K_{sy}L_1y_{c2} - K_{sy}L_1y_{c1} - K_{sy}L_1^2\psi_{c1} - K_{sy}L_1L_3\psi_{c2} \end{aligned} \tag{12}$$

where y_{w1}, y_{w2}, y_b, and y_{c1} represent the lateral displacements of the leading wheelset, trailing wheelset, bogie, and leading car; Ψ_1, Ψ_2, Ψ_b, and Ψ_{c1} represent the yaw angles of the leading wheelset, trailing wheelset, bogie, and leading car; θ_{1L} and θ_{1R} represent the rotation angles of the left and right leading wheels; and θ_{2L} and θ_{2R} represent the rotation angles of the left and right trailing wheels. Here, v is the vehicle travel speed. The other symbols used in the equations are defined in the appendix.

C. FORWARD MOTION OF VEHICLE

The 26 DOF model does not include x-axis direction information (forward motion) because it is derived from the wheelset model (Ψ, y, θ_L, θ_R). The torque used in the 26 DOF model does not cause forward motion; instead, it causes lateral and yaw displacements (y, Ψ). Therefore, this torque can be defined as the centering torque (T_C).

In order to consider the characteristics of the forward motion, the x-axis direction information should be added to each wheel. It significantly complicates the car model. It has to be simplified because real-time calculation is performed. Therefore, the running resistance model (1 DOF) was used. The torque used in this equation can be defined as the traction torque (T_T) because it generates only a forward motion.

III. ACTIVE CONTROL IN IRWS

There are two techniques commonly used to improve the driving performance of railway vehicles. The first technique is a passive method that depends on the design of the wheel shape and stiffness of suspension. However, this technique has several practical constraints because it relies on the structure and properties. In particular, stability and curving performance have always been a difficult tradeoff for design engineers.

The second technique is an active method that controls the actuator or motor. This active method can improve driving performance under various driving conditions compared to passive methods.

This section studies an active control strategy for IRWs, to generate the centering force. RW can passively generate a self-centering force; therefore, no additional control strategy is required except for the traction torque (T_T). However,

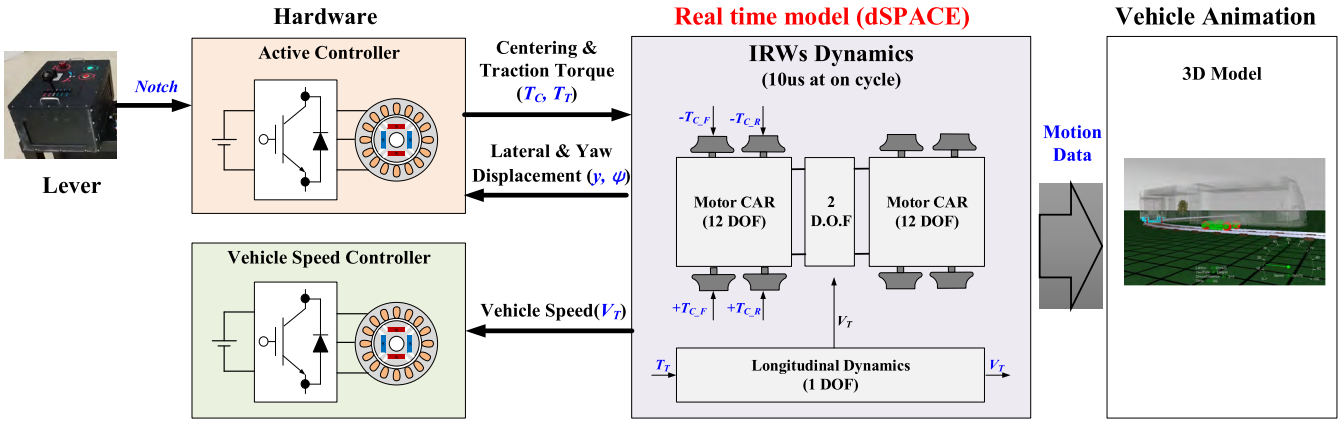

FIGURE 6. Overall configuration of HILS.

in IRWs, it is possible to generate yaw moment by adding the independent wheel torque (T_C) to the existing traction torque control as shown in Fig. 3. This method does not require yaw actuators.

The independent wheel torque control strategy is based on lateral displacement. When $-y$ displacement occurs in the wheelset, the left wheel torque is increased while the right wheel torque is increased in the opposite direction. The difference between the left and right wheel torques produces a clockwise yaw moment, which generates a centering capability as shown in Fig. 4(a). On the other hand, when $+y$ displacement occurs in the wheelset, a yaw moment in the counterclockwise direction is obtained by controlling the wheel torque, as shown in Fig. 4(b). The overall control block diagram is shown in Fig. 5. Similarly, an active control strategy based on yaw displacement can be applied.

The active control requires sensors to measure the lateral or yaw displacement. The sensors must also meet the electrical and mechanical specifications. In particular, they should be reliable under conditions such as vibration, shock, and bad weather. In addition, the mounting position of the sensor and the mechanical interference should also be considered.

TABLE 2. Motor-Inverter specifications for IRWs.

Classification		Contents & Value	Unit
Motor	Type	IPMSM	-
	Poles/slots	6/72	-
	Max torque/power	500/73	Nm/kW
	Base/max speed	1,390/4,450	RPM
	Magnet type	Sm_2Co_{17}	-
	Cooling method	Natural air cooling	-
Inverter	Controller	TMS320F28335	-
	Vdc	750	V
	IGBT spec.	650	A
		1,700	V
	Position sensor	resolver	-
	Switching frequency	4	kHz
	Cooling method	Forced air cooling	-

TABLE 3. Vehicle specifications.

Classification	Contents & Value	Unit
Vehicle type	3 module (tramcars)	-
Wheel type	Independently rotating wheels	-
Gear ratio	1/5.85	
Max wheel torque	2,925	Nm
Distance between wheel flange and rail	6.5	mm

IV. NOVEL HILS SYSTEM

In this section, a novel HILS system is proposed to verify the active control strategy in IRWs. The overall configuration of this system is shown in Fig 6. The proposed HILS configuration consists of a lever, hardware (railway motor & inverter, load motor & inverter), and a real-time tramcar model (dSPACE SCALEXIO).

The notch state of the lever is transmitted to the active controller via CAN communication, where it is converted into a traction torque command. After that, the traction torque and centering torque are transferred from the active controller to the dSPACE, where the dynamical equation of the tramcar is calculated in real time (10 μs at 1 cycles). The dynamic equations consist of 26 DOF and 1 DOF equations, and each equation is calculated through the traction torque and centering torque. The vehicle speed (v) is obtained from the traction torque (T_T) and the running resistance model. The lateral displacement (y) is obtained from the centering torque (T_C) and the 26 DOF model.

The vehicle motion data calculated in dSPACE is transmitted to the vehicle animation. This information is mapped to the 3D vehicle models in real time, so that the vehicle motion can be monitored on the screen.

A detailed diagram of the controller (active controller and vehicle speed controller) and motor–generator set is shown in Fig 7. The load motor is controlled to simulate the vehicle speed. The vehicle speed command calculated from dSPACE is input to the vehicle speed control block. In this block, the speed and current controller are connected in a cascade manner. In the proposed HILS, the centering torque (T_C) changes rapidly to control the lateral displacement. This torque acts as a disturbance to the vehicle speed controller. The disturbance suppression capability of an IP controller is better than that of a PI controller, because an IP controller

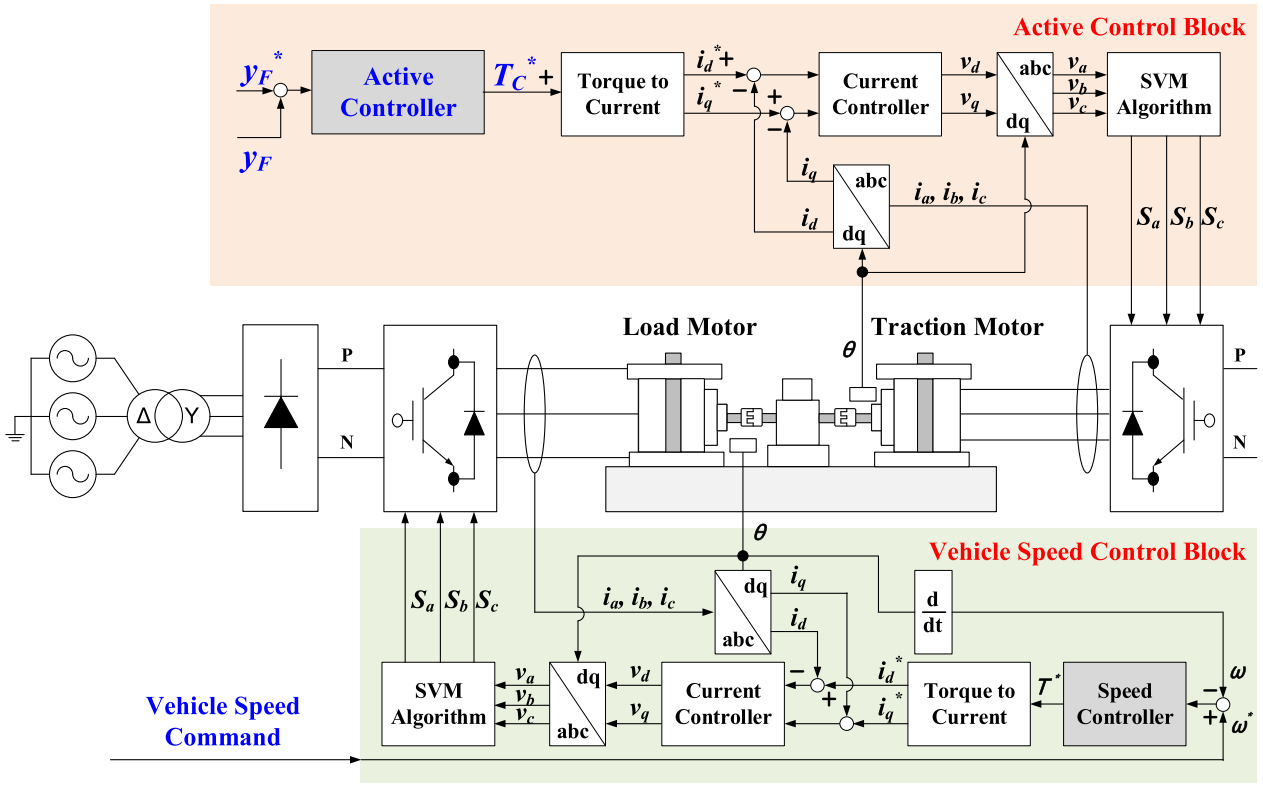

FIGURE 7. Proposed controller and motor-generator set configuration.

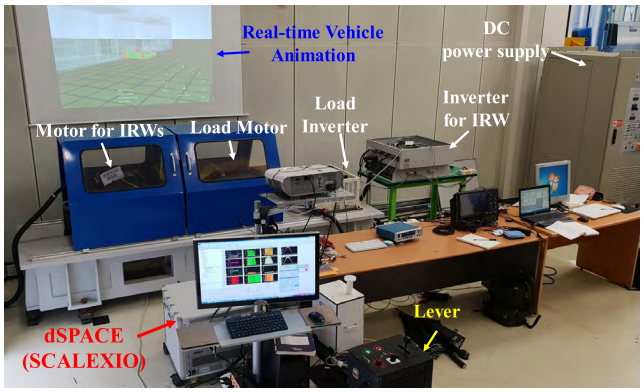

FIGURE 8. The proposed test environment.

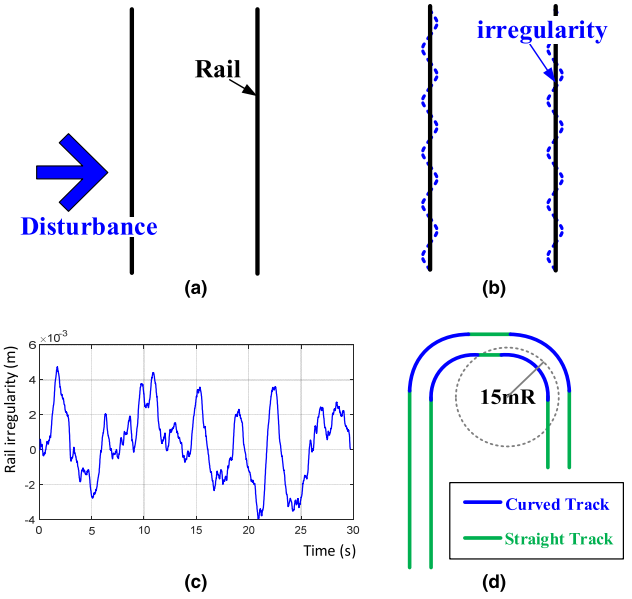

FIGURE 9. Driving condition (a) case 1 (b) case 2 (c) measured irregularity data of case2 (d) case 3.

can increase the bandwidth over that of a PI controller. For this reason, an IP speed controller was adopted.

In an active control block, the traction motor is controlled by the centering torque. In the case of wireless tramcars, voltage fluctuations occur in the battery due to charging and discharging. Therefore, a robust torque control strategy is required considering these driving conditions. For this reason, flux-based torque control is used. The torque command can be easily converted into a current vector by considering the voltage fluctuation [24], [25].

The power for the motor–generator set is supplied from the grid and converted into a DC voltage of 750 V using a transformer and a diode rectifier. Even though a diode rectifier can only supply unidirectional power, the production cost can be reduced. If the DC link of the vehicle inverter and load inverter is connected in common, the power can be circulated according to the motoring and regenerating operations. Therefore, even if a unidirectional power supply is used, four-quadrant operation is possible.

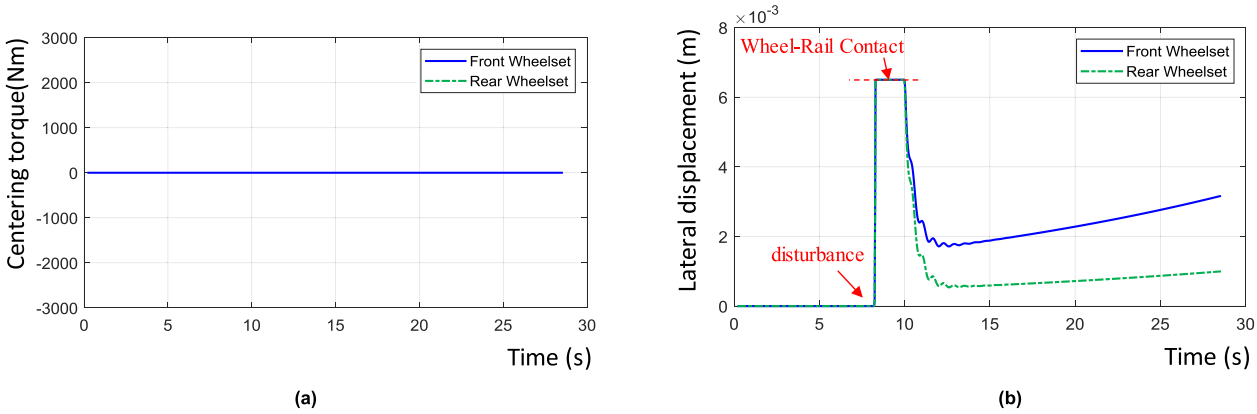

FIGURE 10. Test result under case 1 (without active control) (a) centering torque (b) lateral displacement.

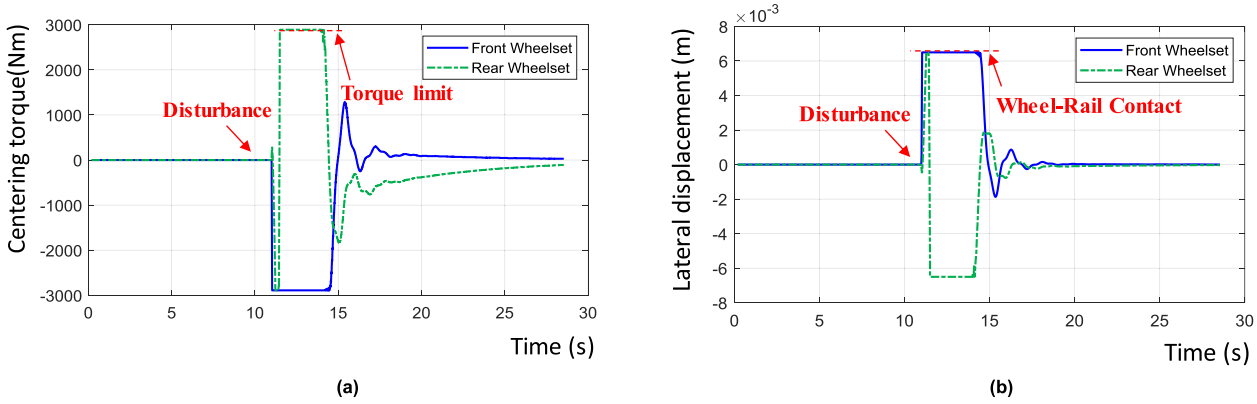

FIGURE 11. Test result under case 1 (with active control) (a) centering torque (b) lateral displacement.

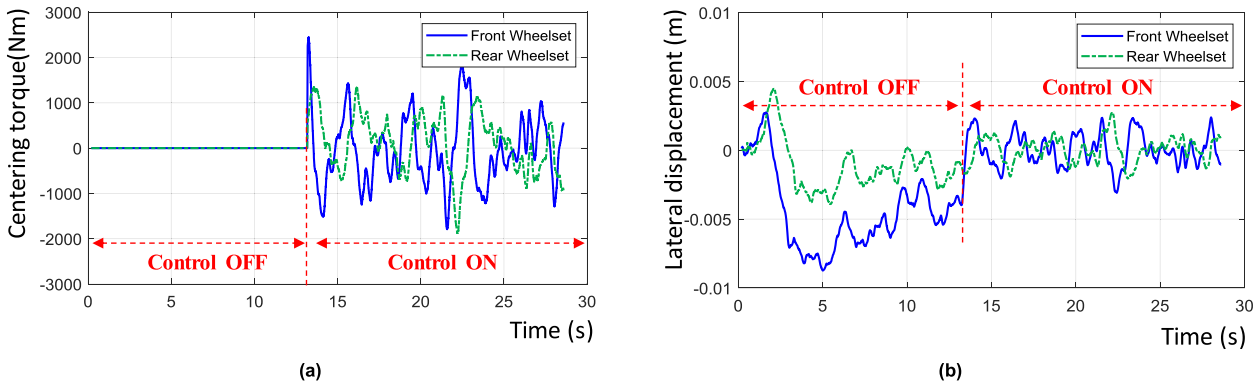

FIGURE 12. Test result under case 2 (a) centering torque (b) lateral displacement.

The specifications of the motor-inverter and vehicle are given in Tables 2 and 3, respectively. The vehicle parameters are given in the appendix. The proposed HILS environment is shown in Fig. 8.

V. TEST SCENARIO

In order to evaluate the performance of the active control, experiments were conducted under three driving conditions.

A. CASE 1. STRAIGHT TRACK (IMPULSE DISTURBANCE)

It is assumed that the track is ideally a straight track and impulse disturbance was generated during driving as shown in Fig 9(a). In order to simulate the disturbance in the tramcar model, we added the $T_{disturb}$ term to (2).

B. CASE 2. STRAIGHT TRACK (RAIL IRREGULARITY)

Since an actual rail will never be a perfectly straight track, there is an irregularity as shown in Fig. 9(b). It acts as a

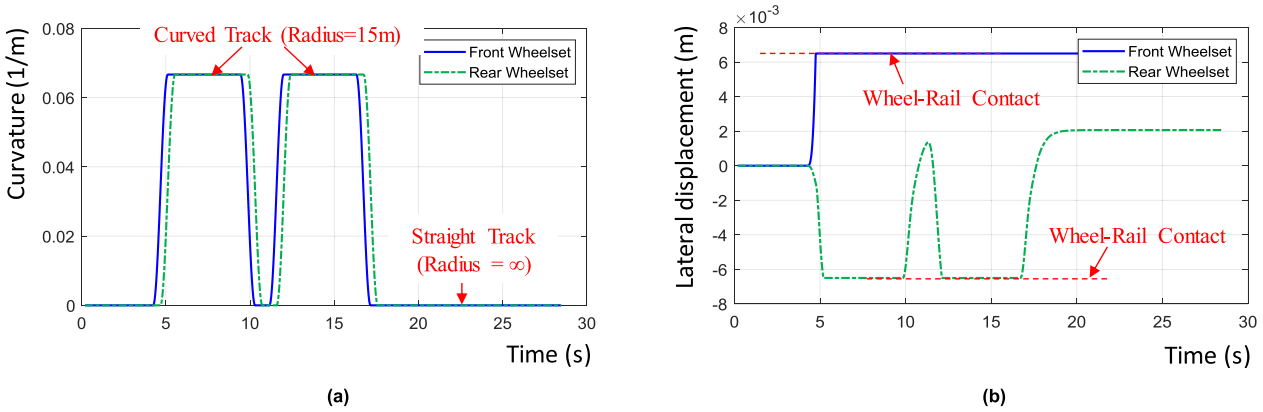

FIGURE 13. Test result under case 3 (without active control) (a) curvature of rail (b) lateral displacement.

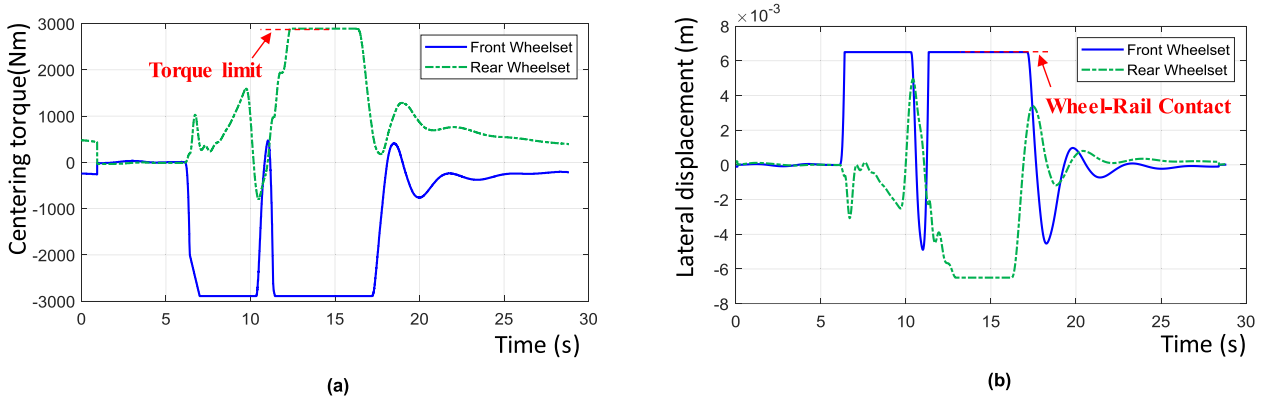

FIGURE 14. Test result under case 3 (with active control) (a) centering torque (b) lateral displacement.

disturbance with a small magnitude and a high frequency. As a result, the lateral displacement gradually increases during driving. The irregularity data of the rail (Fig. 9(c)) was obtained through direct measurements on an actual rail.

C. CASE 3. SHARP CURVED TRACK (15mR)

IRWs have excellent curving capability than RW. However, lateral displacement occurs due to the inertia and centrifugal force of the vehicle when entering a curved track. It creates a large friction between the wheel and the rail. In the test condition of case 3, the track contained both straight and sharp curved portions (radius of curve: 15 m), as shown in Fig. 9(d).

VI. EXPERIMENTAL RESULTS THROUGH HILS

A. CASE 1. STRAIGHT TRACK (IMPULSE DISTURBANCE)

Fig. 10 shows the results of applying only traction torque control (without active control). Lateral displacement occurred due to the impulse disturbance in the straight track. It was limited to ± 6.5 mm due to the mechanical structure of the wheel-to-rail. Even after an impulse disturbance occurs, the wheel does not return to the center of the rail as shown in Fig10. This shows the inherent lack of restoration capability of IRWs when controlling only the traction torque.

Fig. 11 shows the results of the active control based on lateral displacement. When lateral displacement occurs, the centering torque controller is operated. Since the output of this controller generates a torque difference between the left and right wheels (Fig. 11(a)), a restoration capability can be obtained. When a disturbance occurs, it is restored to the center of the rail as shown in Fig. 11(b).

B. CASE 2. STRAIGHT TRACK (RAIL IRREGULARITY)

The results of the active control are shown in Fig. 12. Due to the irregularity in the rail, the lateral displacement gradually increases before the active control. When the active control is activated, the controller outputs a centering torque (Fig. 12(a)). As a result, the lateral displacement decreases (Fig. 12(b)).

C. CASE 3. SHARP CURVED TRACK (15mR)

Fig. 13 shows the results of applying only traction torque control (without active control) under case 3 condition. The change in curvature can be confirmed according to the position of the vehicle (Fig. 13(a)). In a straight track (radius of curve $= \infty$), the vehicle is driven along the center of the rail, but the lateral displacement increases significantly when entering a curved track. However, even when the tramcar

TABLE 4. Parameters of tramcars with IRWs.

Symbol	Quantity	value	Unit
m_w	wheelset mass	778.2	kg
m_b	bogie frame mass	3,900	kg
m_c	car body mass	7,588	kg
I_{wy}	spin moment of inertia of the wheelset	32.774	kg·m^2
I_{wz}	yaw moment of inertia of the wheelset	161.166	kg·m^2
I_{wl}	roll moment of inertia of the wheel	13.745	kg·m^2
I_{tz}	yaw moment of inertia of the bogie frame	4,750	kg·m^2
I_{cz}	yaw moment of inertia of the car body	22,970	kg·m^2
r_0	Wheel radius	0.32	m
a	Half of the truck gauge	0.7175	m
λ	wheel conicity	0.165	
b_1	half of the primary longitudinal spring arm	0.595	m
b_2	half of the secondary longitudinal spring arm	0.622	m
b_3	half of the secondary vertical damping arm	1.15	m
L_1, L_2	half of the primary lateral spring, damping arm	0.9	m
K_{px}, K_{py}	longitudinal and lateral stiffness of the 1st suspension	6,000,000	N/m
C_{px}, C_{py}	longitudinal and lateral damping of the 1st suspension	0	N·s/m
K_{sx}, K_{sy}	longitudinal and lateral stiffness of the 2st suspension	500,000	N/m
C_{sx}	longitudinal damping of the 2st suspension	0	N·s/m
C_{sy}	lateral damping of the 2st suspension	30,000	N·s/m
f_{11}	lateral creep force coefficient	800,000	N
f_{12}	lateral/spin creep force coefficient	3,000	N·m^2
f_{22}	spin creep force coefficient	16	N
f_{33}	longitudinal creep force coefficient	600,000	N
W	axle load	54,085	N

enters a straight track after passing through a curved track, the lateral displacement is not reduced (Fig. 13(b)).

Fig. 14 shows the results of applying active control. Although a high centering torque is required in the curved track, the wheel torque is physically limited by the motor torque and the reduction gear ratio as shown in Fig. 14(a) (500 Nm × 5.85 = 2,925 Nm). Therefore, excellent restoration performance cannot be obtained; however, the contact time between the wheel and the rail (Fig. 14(b)) is highly reduced compared to that in Fig. 13(b). It reduces the flange wear and noise. Moreover, the wheelset is restored to the center of rail after passing through a curved track. This result shows improved curving performance when the active control strategy is applied.

VII. CONCLUSION

In this paper, we studied an active control strategy to improve the driving performance of tramcars with IRWs. Independent torque control of the left and right wheels can generate centering ability without any additional actuator.

A railway vehicle with IRWs has a different platform from that of conventional railway vehicles, which significantly increases the cost of producing the test vehicle. To adapt active control technology for practical use, their feasibility should be verified appropriately. Therefore, it is necessary to develop a test method that reflects the characteristics of the controller and IRWs more accurately.

Most of the existing active control strategies have been validated by using numerical models or scale-vehicles. However, the disadvantage of using such methods is that their similarity with the characteristics of a real vehicle is considerably low. This is one of the obstacles to commercialization.

This study also proposed a novel HILS configuration to validate the active control strategy and to prove the feasibility in a real hardware environment. The vehicle models included longitudinal motion, which was omitted from previous studies. As a result, both the centering torque and traction torque can be considered. The modified vehicle model (27 DOF) was implemented in real time through dSPACE, and the driving test was simulated by linking the real-time model and the motor–generator set.

The active control strategy has excellent centering ability for both straight and curved tracks. It can reduce noise and vibration, and also prevent serious failures such as derailments.

IRWs are suitable for free gauge trains (FGT) and low-floor tramcars that run on tracks with sharp curved tracks. However, IRWs still require a significant amount of research, and the ongoing researches may develop new technologies for replacing the existing RW.

APPENDIX

See Table 4.

REFERENCES

[1] P. Wang, L. Goel, X. Liu, and F. H. Choo, "Harmonizing AC and DC: A hybrid AC/DC future grid solution," *IEEE Power Energy Mag.*, vol. 11, no. 3, pp. 76–83, May/Jun. 2013.
[2] T. J. Blalock, "The rotary era, part 1: Early ac-to-dc power conversion [History]," *IEEE Power. Eng. Mag.*, vol. 11, no. 5, pp. 82–92, Sep./Oct. 2013.
[3] A. Bracciali, "Railway wheelsets: History, research and developments," *Int. J. Railway Technol.*, vol. 5, no. 1, pp. 23–52, 2016.
[4] C. Calleja, López-de-Heredia, H. Gaztañaga, T. Nieva, and L. Aldasoro, "Validation of a modified direct-self-control strategy for PMSM in railway-traction applications," *IEEE Trans. Ind. Electron.*, vol. 63, no. 8, pp. 5143–5155, Aug. 2016.
[5] D. Ronanki, S. A. Singh, and S. S. Williamson, "Comprehensive topological overview of rolling stock architectures and recent trends in electric railway traction systems," *IEEE Trans. Transport. Electrific.*, vol. 3, no. 3, pp. 724–738, Sep. 2017.
[6] P. Pichlik and J. Zdenek, "Locomotive wheel slip control method based on an unscented Kalman filter," *IEEE Trans. Veh. Technol.*, vol. 67, no. 7, pp. 5730–5739, Jul. 2018.
[7] R. Dukkipati, S. N. Swamy, and M. Osman, "Independently rotating wheel systems for railway vehicles-A state of the art review," *Veh. Syst. Dyn.*, vol. 21, no. 1, pp. 297–330, 1992.
[8] J. Pérez, J. M. Busturia, T. X. Mei, and J. Vinolas, "Combined active steering and traction for mechatronic bogie vehicles with independently rotating wheels," *Annu. Rev. Control*, vol. 28, no. 2, pp. 207–217, 2004.

[9] Y. Cho and J. Kwak, "Development of a new analytical model for a railway vehicle equipped with independently rotating wheels," *Int. J. Automot. Technol.*, vol. 13, no. 7, pp. 1047–1056, Dec. 2012.

[10] T. X. Mei and R. M. Goodall, "Wheelset control strategies for a two-axle railway vehicle," in *Proc. 16th IAVSD Symp., Dyn. Veh. Roads Tracks*, Aug./Sep. 1999, pp. 653–664.

[11] T. X. Mei and H. Li, "Control design for the active stabilization of rail wheelsets," *J. Dyn. Syst., Meas., Control*, vol. 130, no. 1, Jan. 2008, Art. no. 011002.

[12] T. X. Mei and R. M. Goodall, "Modal controllers for active steering of railway vehicles with solid axle wheelsets," *Veh. Syst. Dyn.*, vol. 34, no. 1, pp. 25–41, 2000.

[13] T. X. Mei and R. M. Goodall, "Practical strategies for controlling railway wheelsets independently rotating wheels," *J. Dyn. Syst., Meas., Control*, vol. 125, no. 3, pp. 354–360, Sep. 2003.

[14] T. X. Mei and R. M. Goodall, "Robust control for independently rotating wheelsets on a railway vehicle using practical sensors," *IEEE Trans. Control Syst. Technol.*, vol. 9, no. 4, pp. 599–607, Jul. 2001.

[15] Y. Zhao and B. Liang, "Re-adhesion control for a railway single wheelset test rig based on the behaviour of the traction motor," *Veh. Syst. Dyn.*, vol. 51, no. 8, pp. 1173–1185, 2013.

[16] R. M. Goodall and H. Li, "Solid axle and independently-rotating railway wheelsets-A control engineering assessment of stability," *Veh. Syst. Dyn.*, vol. 33, no. 1, pp. 57–67, 2000.

[17] A. J. Powell and A. H. Wickens, "Active guidance of railway vehicles using traction motor torque control," *Veh. Syst. Dyn.*, vol. 25, pp. 573–584, Jan. 1996.

[18] Z.-G. Lu, Z. Yang, Q. Huang, and X.-C. Wang, "Robust active guidance control using the μ-synthesis method for a tramcar with independently rotating wheelsets," *Proc. Inst. Mech. Eng. F, J. Rail Rapid Transit*, vol. 233, no. 1, pp. 33–48, Jan. 2019.

[19] Y. J. Oh, Y. Cho, I.-G. Kim, J. Lee, and H. Lee, "Restoring torque control strategy of IPMSM for the independently rotating wheelsets in wireless trams," *J. Electr. Eng. Technol.*, vol. 12, no. 4, pp. 1683–1689, 2017.

[20] Y. J. Oh, H.-C. Liu, S. Cho, J. H. Won, H. Lee, and J. Lee, "Design, modeling, and analysis of a railway traction motor with independently rotating wheelsets," *EEE Trans. Magn.*, vol. 54, no. 11, Nov. 2018, Art. no. 8205305.

[21] J. H. Won, Y. J. Oh, J. Lee, H. W. Ahn, H. W. Lee, and Y. Cho, "A study on the individual control method comparing the lateral displacement control of front wheel and rear wheel of IRWs system," *IEEE Trans. Appl. Supercond.*, vol. 28, no. 3, Apr. 2018, Art. no. 0601605.

[22] H. Ahn, H. Lee, S. Go, Y. Cho, and J. Lee, "Control of the lateral displacement restoring force of IRWs for sharp curved driving," *J. Electr. Eng. Technol.*, vol. 11, no. 4, pp. 1042–1048, 2016.

[23] S.-Y. Lee and Y.-C. Cheng, "A new dynamic model of high-speed railway vehicle moving on curved tracks," *J. Vib. Acoust.*, vol. 130, no. 1, Nov. 2007, Art. no. 011009.

[24] H. W. de Kock, A. J. Rix, and M. J. Kamper, "Optimal torque control of synchronous machines based on finite-element analysis," *IEEE Trans. Ind. Electron.*, vol. 57, no. 1, pp. 413–419, Jan. 2010.

[25] H. A. A. Awan, Z. Song, S. E. Saarakkala, and M. Hinkkanen, "Optimal torque control of saturated synchronous motors: Plug-and-play method," *IEEE Trans. Ind. Appl.*, vol. 54, no. 6, pp. 6110–6120, Nov./Dec. 2018.

YE JUN OH received the B.S. degree in electrical engineering from Myongji University, South Korea, in 2010, and the M.S. and Ph.D. degrees in electrical engineering from Hanyang University, Seoul, South Korea, in 2012 and 2019, respectively. From 2011 to 2015, he was with Hyundai Mobis, Yongin, South Korea. His research interest includes motor design and applications of motor drive, such as electric vehicles and railway propulsion systems.

JAE-KWANG LEE received the B.S. degree in electrical engineering from Kunsan National University, Kunsan, South Korea, in 2014, and the M.S. degree in electrical engineering from Hanyang University, Seoul, South Korea, in 2016, where he is currently pursuing the Ph.D. degree with the Department of Electrical Engineering. His research interests include design, analysis, and testing and control of motor/generator, power conversion systems, and applications of motor drive.

HUAI-CONG LIU was born in Wuhan, China, in 1988. He received the B.S. degree in electrical engineering from Chungnam National University, Daejeon, South Korea, in 2012, and the Ph.D. degree in electrical engineering from Hanyang University, Seoul, South Korea, in 2018. Since 2018, he has been a Research Professor with the Department of Electrical Engineering, Hanyang University, Seoul, South Korea. He is currently researching electric machinery and drives, and the electromagnetic design of motors and generators. He is also interested in the applications of mechatronics systems in robotics, automotive parts, and electric vehicles.

SOOYOUNG CHO received the B.S. degree in electrical engineering from Myongji University, Yongin, South Korea, in 2013, and the M.S. degree in electrical engineering from Hanyang University, Seoul, South Korea, in 2015, where she is currently pursuing the Ph.D. degree with the Department of Electrical Engineering. Her research interests include design, analysis, and testing and control of motor/generator, power conversion systems, and applications of motor drive.

JU LEE (SM'05) received the M.S. degree from Hanyang University, Seoul, South Korea, in 1988, and the Ph.D. degree in electrical engineering from Kyusyu University, Japan, in 1997. He joined Hanyang University, in 1997, where he is currently a Professor with the Division of Electrical and Biomedical Engineering. His main research interests include electric machinery and its drives, electro-magnetic field analysis, transportation systems, such as hybrid electric vehicles (HEV), and railway propulsion systems. He is a member of the IEEE Industry Applications Society, the Magnetics Society, and the Power Electronics Society.

HO-JOON LEE was received the M.S. and Ph.D. degrees in electrical engineering from Hanyang University, Seoul, South Korea, in 2011 and 2015, respectively. He has been an Assistant Professor with the Department of Electric Automatization, Busan Institute of Science and Technology (BIST), since 2015. His research interests include design, analysis, testing and control of motor/generator, power conversion systems, and applications of electric machinery.